Investigating Narrow Plasmons in Nanoparticle Arrays Fabricated Using Electron Beam Lithography.

Erin M. Hicks[*§], Linda Gunnarrsson[†], Tomas Rindevicius[†], Shengli Zou[*], Bengt Kasemo[†], Mikael Käll[†], Goerge C. Schatz[*], Kenneth G. Spears[*], and Richard P. Van Duyne[*]

*Department of Chemistry, Northwestern University, Evanston, IL 60208-3113 USA
† Department of Applied Physics, Chalmers University of Technology, Göteborg, Sweden S-214 96
§ Corresponding Author: e-mclellan@northwestern.edu

ABSTRACT

The improvement of nanofabrication is one of the driving forces behind advancements in the fields of electronics, photonics and sensors. Precise control over nanoscale architecture is an essential aspect in relating new size-dependent material properties. Direct writing methods such as Electron Beam Lithography (EBL), enable precise "user-defined" writing of nanostructures in a wide range of materials. Using electrodynamics calculations, Schatz and coworkers have discovered one dimensional array structures built from spherical silver nanoparticles that produce remarkably narrow plasmon resonance spectra upon irradiation with light that is polarized perpendicularly to the array axis. In order to investigate these interactions, precise control of nanoparticle orientation, size, shape and spacing is necessary. If the overall structures have excessive defects then the effect may not be seen. To have the best control over array fabrication and to look at these interactions experimentally, EBL was used to construct lines of circular cylinders of varying interparticle spacings. Dark field microscopy was used to look at overall sample homogeneity and collect the single particle plasmon resonance spectrum. Additionally, a UV-visible spectrometer with a variable angle stage was used to look at the bulk line properties. With experimental verification of the theory will lead to not only a more thorough understanding of the underlying principles of nanophotonics, but also application in biosensing, that potentially improve on current technologies.

INTRODUCTION

Assemblies of nanoparticles often can be used to provide special functionalities that are important in sensing [1], optical waveguides [2], and filters [3]. The use of assemblies, rather than single particles, offers the ability to average a signal across several similar particles (increasing intensity and eliminating discrepancies caused by defects) and the miniaturizing equipment is much simpler. Since the design of a practical plasmonic nanodevice relies heavily on arrays of noble metal nanoparticles, the interactions between these nanoparticles is a crucial and often overlooked design parameter. These interactions can be either short or long range for a variety of structure types including both highly dense array structures [4, 5] and individual pairs of nanoparticles [6]. They can be measured and studied by observing changes in the LSPR peak shape and position. Theoretical calculations also show these unique interactions. For example, previous work by Schatz et al. has predicted narrowed plasmon peaks in two-dimensional [7] and one-dimensional arrays [8, 9, 10] as a result of diffractive interactions between the

particles. For one-dimensional chains of particles above a critical size and with polarization and wave vectors taken to be perpendicular to the array axis, narrow peaks with widths less than 1 nm were reported. The narrow peaks are caused by the coherent interactions between the particles when the incident wavelength is close to the interparticle distance. [8, 10] By taking advantage of these coherent interactions, it is possible to create nanodevices with narrow lines that could lead to better sensing capabilities than are possible with isolated metal particles or aggregates of particles.

Methods for preparing nanoparticle arrays vary as widely as their uses. Standard lithographic techniques can be broken into two major categories, direct-write methods and natural lithographies. Natural lithographies, including nanosphere lithography [11, 12], are massively parallel and offer an inexpensive and rapid method for fabricating a large array of nanostructured materials. They, however, are limited by restricted lattice/inter-particle spacings, shapes, and sizes that can be produced, as well as a large range of defects that occur in the structure. On the other hand, direct write methods, such as photolithography [13], dip-pen lithography [14], and electron beam lithography (EBL) [15], offer fine control of size, shape, and lattice spacing, as well as few defects. Of the major problems associated with direct write methods are the serial nature of the process and the higher cost associated with production of arrays. EBL was chosen for this project because fine control over sample morphology was crucial (based on theoretical modeling) to whether or not the sharp plasmon was going to be observed.

EXPERIMENTAL DETAILS

Materials

Ag (99.99%) purchased from D.F. Goldsmith (Evanston, IL) and . Au (99.99%) was purchased from .Tungsten vapor deposition boats were purchased from R.D. Mathis (Long Beach, CA). Glass substrates were 25mm by 25mm, no. 2 cover slips from Fisher Scientific (Pittsburgh, PA). Pretreatment of the glass substrates required H2SO4, H2O2, and NH4OH, and the resist developer, hexylacetate were all obtained from Aldrich Chemicals. The resist, ZEP 520 was purchased from Nippon ZEON Ltd. Shipley Remover 1165 was purchased from Microchem Inc.

Array Fabrication

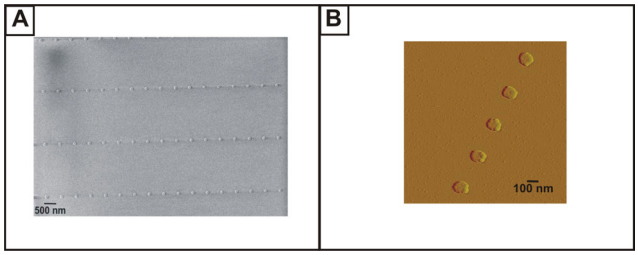

Figure 1. (A) An SEM image taken of a pad of particles on glass with a spacing of 632 nm, diameter = 130 nm, height = 30 nm. (B) AFM image of a few Ag nanoparticles on glass. Height = 31.33 ± 1.3 nm, width = 133 ± 2.2 nm.

The samples were prepared by EBL on cleaned number 2 cover glass slips. After cleaning the glass was spin-coated (6000 rpm, 1 min) with a 60 nm thin film of an electron-sensitive resist, ZEP 520 diluted 1:2 in aniline. Before the pattern was exposed, the resist film was coated resistively with a 10 nm thin film of gold to make the surface conductive. The resolution of the EBL system used (JEOL JBX5D-II) is approximately 20

nm, employing an accelerating voltage of 50 kV. After exposure, the Au film was removed by etching in an aqueous. The patterns were then developed in hexylacetate, creating a patterned resist film on top of which silver was deposited in a high-vacuum thin film vapor deposition system (AVAC HVC 600). The resist was dissolved in a strong solvent (Shipley Remover 1165), which also removes the metal deposited on the top of the resist. To ensure that the metal film on top of the resist does not have any physical contact with the metal deposited directly on the substrate (Figure 1A and 1B).

Optical Measurements

All optical measurements were made using an inverted microscope (Eclipse TE300, Nikon Instruments) and a fiber coupled to a miniature grating spectrometer (AvaSpec 2048, Avantes). The scattering measurements reported here were recorded over the range 350-850 nm. White light from the TE300 lamp was collimated before being passed through the sample. The scattered light was collected with a 60x objective. A color video camera was also attached to the front port to collect optical images of the particle lines. A dark-field condenser was used to collect the light scattered by the nanoparticle lines.

Scanning Electron Microscopy (SEM) and Atomic Force Microscopy (AFM)

AFM images were collected using a Digital Instruments Nanoscope III microscope operated in tapping mode using etched Si nanoprobe tips (Digital Instruments, Santa Barbara, CA). These tips have resonance frequencies between 280 and 320 kHz and are conical shape with a cone angle of 20° and an effective radius of curvature at the tip of 10 nm. SEM images were obtained using a Gemini LEO 550 (Japan), with an accelerating voltage of 1 keV and an average working distance of 4 mm.

RESULTS AND DISCUSSION

Figure 2 shows that for the index matched samples, there is a shoulder on the red side of the single particle plasmon whose wavelength varies with particle spacing. The particles in Fig. 2A have a diameter of 130 nm and a height of 30 nm. The single particle spectrum for these particles are included as a

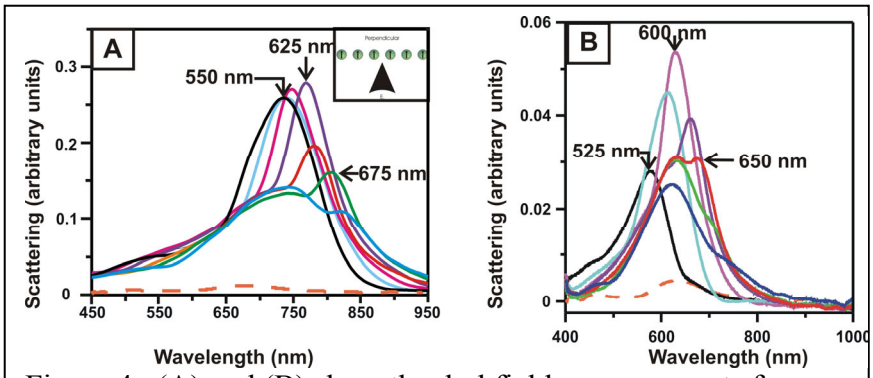

Figure 4. (A) and (B) show the darkfield measurements for samples with 2 um, diameter = 130 nm and 5 um, diameter = 100 nm spacing between lines respectively taken of arrays varying in spacing from 400 to 700 nm with a uniform refractive index (RI = 1.5)around the particles. Both (A) and (B) were collected with a 60x objective. The inset in (A) is the excitation geometry of the particles for both sets of measurements. Corresponding single particle spectra for each case are included (dashed line).

dashed line. For a separation of 550 nm, the peak (λ_{max}= 740 nm) has low intensity and FWHM of approximately 125 nm. As the interparticle distance increases the shoulder on the red portion of the lineshape redshifts, narrows and becomes more intense, with a maximum intensity occurring at a spacing of 625 nm (λ=780 nm, FWHM = 60 nm). For still larger spacings, the peak remains narrow, but decreases in intensity until it is no longer observed in the spectrum. The narrow shoulder also occurs in arrays with larger column spacings (5 μm) and slightly smaller particles (100 nm), as seen in Figure 2B. The progression of plasmon peaks is the same as above: below the optimal spacing the plasmon peak is low in intensity and broad (FWHM = 100 nm, 525 nm spacing), at the optimal spacing of 600 nm there is a shoulder whose FWHM is 50 nm, and above the optimal spacing the shoulder decreases in intensity and eventually disappears altogether. The spectra in 2B are blue shifted from those in 2A due to the smaller particle size. When collecting with other objectives (i.e. 10×), the property can still be seen (data not shown).

In the earlier theory study only the extinction spectra were calculated. Because of the weak signals produced by the arrays it was necessary to use Rayleigh scattering spectroscopy rather than extinction, so in the present studies we have calculated the scattering spectra for one and two-dimensional arrays of silver nanoparticles to simulate the measurements. First, the periodic discrete dipole approximation DDA method described previously was used to generate results for two-dimensional rectangular arrays of 130 nm diameter particles each with height 30 nm and with a 2 μm distance between each column. The results for a spacing of 600 nm (not shown) were compared with one-dimensional chain results, and only small differences were found, so additional calculations only considered the one-dimensional chains. The additional calculations involve varying the interparticle distance from 500 nm to 700 nm, with a cylinder height of 30 nm and particle diameter of either 100

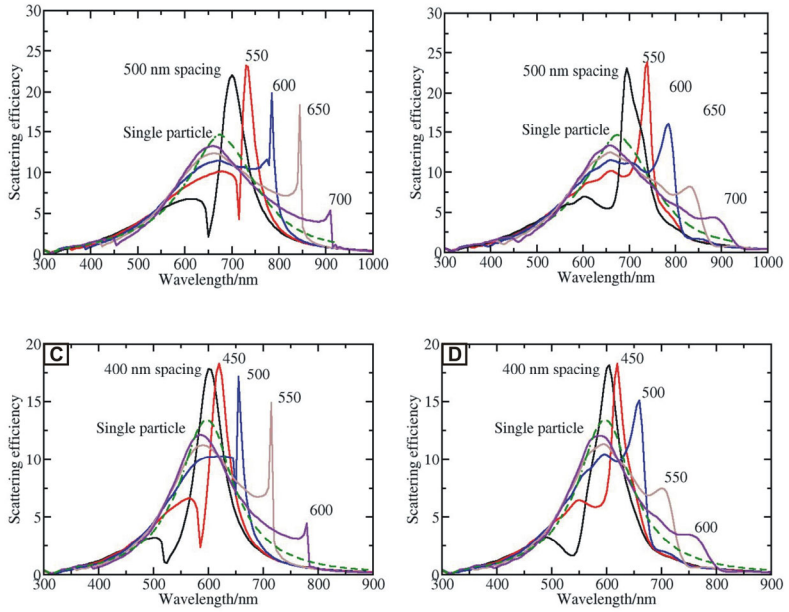

Figure 5. (A) Scattering efficiencies for a chain of 500 cylinders with height of 30 nm and diameter of 130 nm. (B) Scattering efficiencies for a chain of 20 cylinders with height of 30 nm and diameter of 130 nm. (C) Scattering efficiencies for a chain of 500 cylinders with height of 30 nm and diameter of 100 nm. (D) Scattering efficiencies for a chain of 20 cylinders with height of 30 nm and diameter of 100 nm. Corresponding single particle spectra for each case are included (dashed line).

or 130 nm. The calculations considered 500 particles in which both polarization and wave vectors are perpendicular to the array axis. The index of refraction of the medium is taken to be 1.3, as this gives a better match to the spacing dependence of the diffractively coupled results than does 1.5 (from which we infer that the effective refractive index in the experiments is 1.3). The results for the 130 nm particles are presented in Figure 3A, along with the corresponding single particle spectrum. The figure shows resonance wavelengths and variation with spacing that are in good agreement with the observations. However the shoulder on the red portion of the plasmon band is much narrower than in the experiments, with widths as small as 2 nm when the interparticle spacing is 650 nm. Fig. 3B shows that if only adjacent groups of 20 particles in the 500 particle chain are allowed to couple, the widths are in reasonable agreement with the measured results in Fig. 2A. Figs. 3C and 3D show analogous results for the 100 nm diameter particle, and again we see that the results when only 20 adjacent particles are allowed to couple (Fig. 3D) that best match the experiments in Fig. 2B. The good agreement for reduced coherent coupling between the particles likely mimics the influence of the incoherent light source used to excite the particles, as well as the influence of defects, lattice imperfections and local variations in the index of refraction.

CONCLUSION

In summary, this work provides the first demonstration of diffractively narrowed plasmon excitation in columnar arrays of particles, following up the earlier predictions of theory. Critical factors to the success of this experiment are the use of a dark field configuration, a uniform refractive index and high sample quality. By varying the interparticle spacing from 350-800 nm, the diffractively narrowed peak grows into the plasmon spectrum, reaches a maximum and then decreases in intensity and eventually disappears. Also presented are theoretical calculations that support the experimental data. EBL has provided the ideal tool to make multiple sample areas on a substrate with precise control over particle size and spacing. By showing experimental evidence for diffractively narrowed plasmon line shapes, the design of new devices to improve the diffractive response should be possible.

ACKNOWLEDGEMENTS

Funding for this work was provided by NSEC program of the NSF (EEC-0118025) and the Swedish Research Council (contract no. 2001-2672). The authors acknowledge Dr. Christy Haynes for initiating the collaboration between the groups to make this work possible. EH thanks Dr. Yury Alavardyan, Katarina Logg, and Chanda R. Yonzon for the help and valuable discussions.

REFERENCES

1. A. J. Haes, R. P. Van Duyne, *J. Am. Chem. Soc.,* **124**, 10596-10604 (2002).
2. W. Knoll, *Ann. Rev. Phys. Chem.*, ***49***, 569-638 (1998).
3. Y. Dirix, C. Bastiaansen, W. Caseri, P. Smith,*Adv. Mater.*, **11**, 223-227 (1999).

4. A. J. Haes, S. L. Zou, G. C. Schatz, R. P. Van Duyne, *J. Phys. Chem. B*, **108**, 109-116 (2004).
5. A. J. Haes, S. L. Zou, G. C. Schatz, R. P. Van Duyne, *J. Phys. Chem. B*, **108**, 6961-6968 (2004).
6. L. Gunnarsson, T. Rindzevicius, J. Prikulis, B. Kasemo, M. Kall, S. L. Zou, G. C. Schatz, *J. Phys. Chem. B* , **109**, 1079-1087 (2005).
7. S. Zou, G. C. Schatz, *J. Chem. Phys*, **121**, 12606-12612 (2004).
8. S. Zou, N. Janel, G. C. Schatz, *J. Chem. Phys* , **120**, 10871-10875 (2004).
9. S. Zou,; G. C. Schatz, SPIE Proceedings, **5513**, 22-29 (2004)**.**
10. S. Zou, G. C. Schatz, *J. Chem. Phys.*, *In Press* (2005).
11. J. C. Hulteen, C. R. Martin, *J. Mater. Chem.*, **7**, 1075 – 1087 (1997).
12. C. L. Haynes, R. P. Van Duyne, *J. Phys. Chem. B*, **105**, 559-5611 (2001).
13. O. J. Martin, *Micronelectron. Eng.*, **67-68**, 24-30 (2003).
14. R. D. Piner, J. Zhu, F. Xu, S. Hong, C. A. Mirkin, *Science*, **283**, 661-663 (1999).
15. C. L. Haynes, A. D. McFarland, L. L. Zhao, G. C. Schatz, R. P. Van Duyne, L. Gunnarsson, J. Prikulis, B. Kasemo, M. Kall, *J. Phys. Chem. B* , **107**, 7337-7342 (2003).